

# Inclusive and exclusive diffractive production of dilepton pairs in proton-proton collisions at high energies

G. Kubasiak<sup>1,\*</sup> and A. Szczurek<sup>1,2,†</sup>

<sup>1</sup>*Institute of Nuclear Physics PAN, PL-31-342 Cracow, Poland*

<sup>2</sup>*University of Rzeszów, PL-35-959 Rzeszów, Poland*

(Dated: November 23, 2018)

## Abstract

We calculate for the first time cross sections for single and central diffractive as well as exclusive diffractive production of dilepton pairs in proton-proton collisions. Several differential distributions are shown. The inclusive diffractive processes are calculated using diffractive parton distributions extracted from the analysis of diffractive structure function and dijet production at HERA. We find that the inclusive single-diffractive Drell-Yan process is by about 2 orders of magnitude smaller than ordinary Drell-Yan process. The central-diffractive processes are smaller by one order of magnitude compared to single-diffractive ones. We consider also exclusive production of dilepton pairs. The exclusive photon-pomeron (pomeron-photon) process constitutes a background to the QED photon-photon process proposed to be used for controlling luminosity at LHC. Both processes are compared then in several differential distributions. We find a region of the phase space where the photon-pomeron or pomeron-photon contributions can be larger than the photon-photon one.

PACS numbers: 12.40.-y, 13.60.-r, 13.85.Qk

---

\* Gabriela.Slipek@ifj.edu.pl

† Antoni.Szczurek@ifj.edu.pl

## I. INTRODUCTION

The Drell-Yan production process is often used to extract quark and antiquark distributions in the nucleon. Next to open heavy quark production associated with heavy-flavour semileptonic decays it is one of the most important mechanisms for inclusive production of leptons. At large lepton rapidity the Drell-Yan process may be very sensitive to the gluon distributions at small- $x$  [1]. Can the diffractive mechanisms contribute to this region too?

The diffractive processes were intensively studied in  $ep$  collisions at HERA. A formalism has been developed how to calculate them in terms of the diffractive structure functions. The situation in proton-proton collisions is more complicated. The single production diffractive cross sections in proton-proton collisions constitute usually less than 5 % of standard inclusive cross sections. They were calculated for  $W$  and  $Z$  boson [2], dijet [3], open  $c\bar{c}$  [4] as well as for Higgs [5]. It was shown that a naive Regge factorization leads to a sizeable overestimation of the cross section and additional absorption mechanism must be included. Central diffractive processes were calculated only for jet [6],  $c\bar{c}$  [7] and  $Z^0$  [8]. Here we wish to calculate their contribution for dilepton production. In this context we will use diffractive parton distributions found by the H1 Collaboration in the analysis of proton diffractive structure function  $F_2^{(D)}$  as well as dijet production in DIS [9].

It was discussed several times in the literature that the double-photon production of dileptons in the  $pp \rightarrow pp l^+ l^-$  reaction can be considered as a luminosity monitor for LHC [10]. Recently we have studied the mechanism of dilepton production in  $\gamma p \rightarrow l^+ l^- p$  via exchange of gluonic ladder [11]. The same mechanism can be used in proton-proton collisions when the photon is in the intermediate state and couples to the parent nucleon through the proton electromagnetic form factor(s). It is therefore of interest how this mechanism competes with the photon-photon mechanism suggested as the luminosity monitor. We think therefore that the evaluation of the cross section for the diffractive exclusive mechanism is very important in this context. We wish to make first predictions of the cross section for the diffractive exclusive mechanism. We will present several differential distributions in order to understand the competition of the diffractive mechanism with the QED one. We will try to identify regions of phase space where the diffractive mechanism may dominate over the QED mechanism which can be helpful in its experimental identification.

This paper is organized as follows, In Sec.II we present a formalism used to calculations of diffractive processes and results obtained for single and double diffractive Drell-Yan mechanism for  $\sqrt{s} = 500, 1960, 14000$  GeV energy. In Sec.III we recall a formalism which was used to calculate the amplitude  $\mathcal{M}(\gamma p \rightarrow \gamma^*(q^2)p)$  as well as we present a formalism for the  $pp \rightarrow pl^+ l^- p$  reaction both via photon-photon fusion and via photon-pomeron (pomeron-photon) fusion. Next, we compare the results for both contributions. The last section summarizes our paper.

## II. INCLUSIVE DIFFRACTIVE PRODUCTION OF DILEPTONS

### A. Formalism

The mechanisms of the ordinary as well as diffractive production of dileptons are shown in Figs.1,2,3.

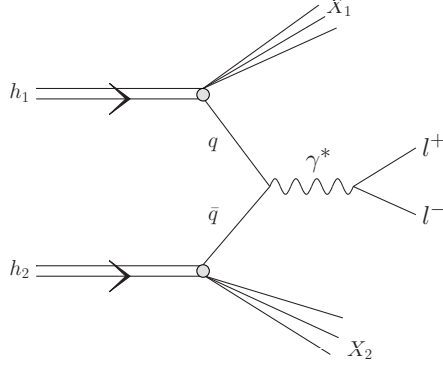


FIG. 1. The ordinary leading-order Drell-Yan mechanism of the lepton pair production.

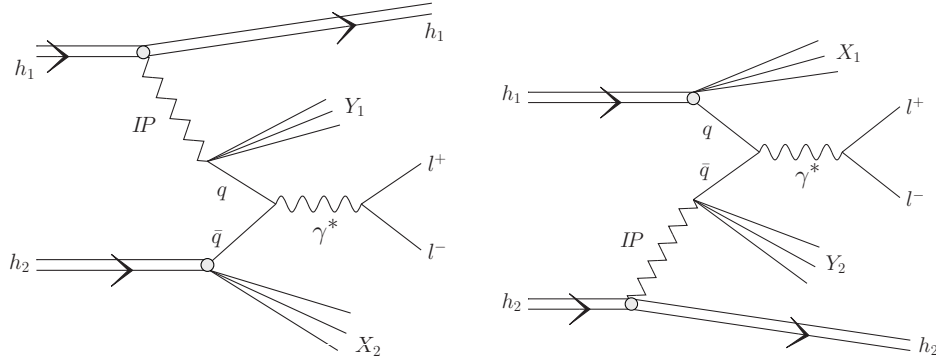


FIG. 2. The mechanism of single-diffractive production of dileptons.

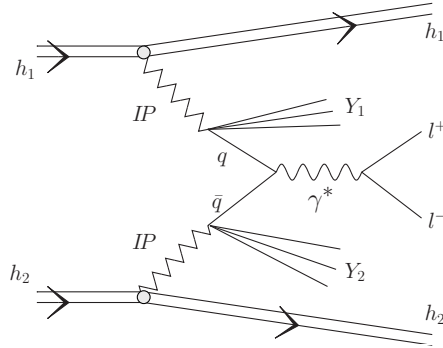


FIG. 3. The mechanism of central-diffractive production of dileptons.

In the following we apply the Ingelman and Schlein approach [3]<sup>1</sup>. In this approach one assumes that the Pomeron has a well defined partonic structure, and that the hard process takes place in a Pomeron–proton or proton–Pomeron (single diffraction) or Pomeron–Pomeron (central diffraction) processes. We calculate triple differential distributions

$$\frac{d\sigma_{DY}}{dy_1 dy_2 dp_t^2} = K \frac{|M|^2}{16\pi^2 \hat{s}^2} \left[ \left( x_1 q_f(x_1, \mu^2) x_2 \bar{q}_f(x_2, \mu^2) \right) + \left( x_1 \bar{q}_f(x_1, \mu^2) x_2 q_f(x_2, \mu^2) \right) \right], \quad (2.1)$$

<sup>1</sup> In the literature also dipole model was used to estimate diffractive processes [12].

$$\frac{d\sigma_{SD}}{dy_1 dy_2 dp_t^2} = K \frac{|M|^2}{16\pi^2 \hat{s}^2} \left[ \left( x_1 q_f^D(x_1, \mu^2) x_2 \bar{q}_f(x_2, \mu^2) \right) + \left( x_1 \bar{q}_f^D(x_1, \mu^2) x_2 q_f(x_2, \mu^2) \right) \right], \quad (2.2)$$

$$\frac{d\sigma_{CD}}{dy_1 dy_2 dp_t^2} = K \frac{|M|^2}{16\pi^2 \hat{s}^2} \left[ \left( x_1 q_f^D(x_1, \mu^2) x_2 \bar{q}_f^D(x_2, \mu^2) \right) + \left( x_1 \bar{q}_f^D(x_1, \mu^2) x_2 q_f^D(x_2, \mu^2) \right) \right] \quad (2.3)$$

for ordinary, single-diffractive and central-diffractive production, respectively. The matrix element squared for the  $q\bar{q} \rightarrow l^+ l^-$  process reads

$$\left| M(q\bar{q} \rightarrow l^+ l^-) \right|^2 = 32\pi^2 \alpha_{em}^2 \frac{(m_l^2 - \hat{t})^2 + (m_l^2 - \hat{u})^2 + 2m_l^2 \hat{s}}{\hat{s}^2}.$$

In this approach longitudinal momentum fractions are calculated as

$$\begin{aligned} x_1 &= \frac{m_t}{\sqrt{s}} \left( e^{y_1} + e^{y_2} \right), \\ x_2 &= \frac{m_t}{\sqrt{s}} \left( e^{-y_1} + e^{-y_2} \right) \end{aligned} \quad (2.4)$$

with  $m_t = \sqrt{(p_t^2 + m_l^2)} \approx p_t$ . The distribution in the dilepton invariant mass can be obtained by binning differential cross section in  $M_{l^+ l^-}$ .

We do not calculate the higher-order Drell-Yan contributions and include them effectively with the help of a so-called  $K$ -factor. We have checked that this procedure is precise enough in the case of ordinary Drell-Yan. The  $K$ -factor for the Drell-Yan process can be calculated as [13]

$$K = 1 + \frac{\alpha_s}{2\pi} \frac{4}{3} \left( 1 + \frac{4}{3} \pi^2 \right).$$

Here the running coupling constant  $\alpha_s = \alpha_s(\mu^2)$  is evaluated at  $\mu^2 = M_{l^+ l^-}^2$ .

The 'diffractive' quark distribution of flavour  $f$  can be obtained by a convolution of the flux of Pomerons  $f_{\mathbf{P}}(x_{\mathbf{P}})$  and the parton distribution in the Pomeron  $q_{f/\mathbf{P}}(\beta, \mu^2)$ :

$$q_f^D(x, \mu^2) = \int dx_{\mathbf{P}} d\beta \delta(x - x_{\mathbf{P}} \beta) q_{f/\mathbf{P}}(\beta, \mu^2) f_{\mathbf{P}}(x_{\mathbf{P}}) = \int_x^1 \frac{dx_{\mathbf{P}}}{x_{\mathbf{P}}} f_{\mathbf{P}}(x_{\mathbf{P}}) q_{f/\mathbf{P}}\left(\frac{x}{x_{\mathbf{P}}}, \mu^2\right). \quad (2.5)$$

The flux of Pomerons  $f_{\mathbf{P}}(x_{\mathbf{P}})$  enters in the form integrated over four-momentum transfer

$$f_{\mathbf{P}}(x_{\mathbf{P}}) = \int_{t_{min}}^{t_{max}} dt f(x_{\mathbf{P}}, t), \quad (2.6)$$

with  $t_{min}, t_{max}$  being kinematic boundaries.

Both pomeron flux factors  $f_{\mathbf{P}}(x_{\mathbf{P}}, t)$  as well as quark/antiquark distributions in the pomeron were taken from the H1 collaboration analysis of diffractive structure function and diffractive dijets at HERA[9]. The factorization scale for diffractive parton distributions is taken as  $\mu^2 = M_{ll}^2$ .

## B. Absorption corrections

Up to now we have assumed Regge factorization which is known to be violated in hadron-hadron collisions. It is known that soft interactions lead to an extra production of particles which fill in the rapidity gaps related to pomeron exchange.

Different models of absorption corrections (one-, two- or three-channel approaches) for diffractive processes were presented in the literature. The absorption effects for the diffractive processes were calculated e.g. in [8, 14, 15]. The different models give slightly different predictions. Usually an average value of the gap survival probability  $\langle |S|^2 \rangle$  is calculated first and then the cross sections for different processes is multiplied by this value. We shall follow this somewhat simplified approach also here. Numerical values of the gap survival probability can be found in [8, 14, 15]. The survival probability depends on the collision energy. It is sometimes parametrized as:

$$\langle |S|^2 \rangle (\sqrt{s}) = \frac{a}{b + \ln(\sqrt{s})} . \quad (2.7)$$

The numerical values of the parameters can be found in original publications. As discussed in [8, 14] the absorptive corrections for single and central diffractive DY are somewhat different.

## C. Results

In this section we shall present several differential distributions for the inclusive diffractive production of the dilepton pairs. Let us start from the presentation of one-dimensional distributions.

In the presentation below we shall show results for dimuon production. The cross sections for dielectrons are larger within the line thickness. In Fig.4 we show invariant mass distributions of dilepton pair. We compare contributions of diffractive and ordinary Drell-Yan processes. The single diffractive distributions are smaller than that for the ordinary Drell-Yan by a factor 10. The calculation done assumes Regge factorization. Absorption corrections, i.e. Regge factorization violation, can be taken into account by a multiplicative factor being a probability of a rapidity gap survival (see e.g.[8]). Such a factor is approximately  $S_G = 0.2$  for the RHIC energy  $\sqrt{s} = 500$  GeV,  $S_G = 0.1$  for the Tevatron energy  $\sqrt{s} = 1960$  GeV and  $S_G = 0.05$  for the LHC energy  $\sqrt{s} = 14$  TeV. The diffractive distributions shown should be multiplied in addition by these factors. In order to avoid model dependence we shall include them only when comparing different contributions (the reader can use his/her own numbers).

In Fig.5 we show the ratios of the cross sections of diffractive (single and central) to the ordinary Drell-Yan for different energies  $\sqrt{s} = 500, 1960, 14000$  GeV. We did not include here the gap survival factors which are model dependent. The ratios for single-diffractive DY is almost independent of dilepton mass whereas that for central-diffractive DY slightly decreases with the dilepton mass. The result found here differs from that found in the dipole approach in Ref.[12]. In addition the ratio for the single-diffractive component is almost energy independent (please note that here we have not included the gap survival factor which decreases logarithmically with energy). This evident difference between our approach and the dipole approach requires a deeper understanding in the future.

In Fig.6 we show distribution in transverse momentum of individual leptons for diffractive contributions at  $\sqrt{s} = 500, 1960, 14000$  GeV. For comparison we show also prediction for the ordinary Drell-Yan contribution. A somewhat strange shape for  $p_t \in (0-1)$  GeV is a

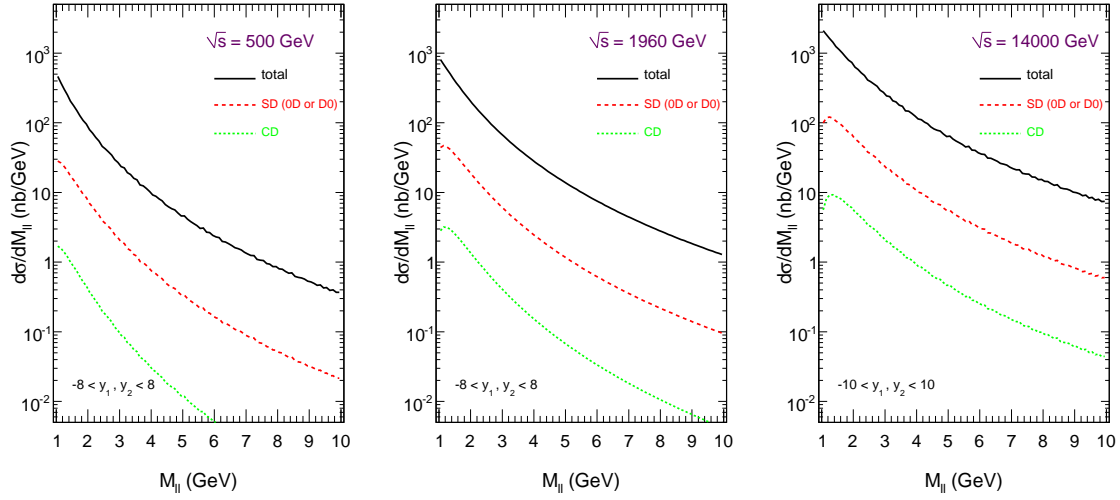


FIG. 4. Invariant mass ( $M_{ll}$ ) distributions for the ordinary Drell-Yan (black line), single diffractive DY (dashed, red online) and central diffractive DY (dotted green online). The results are shown for energies  $\sqrt{s} = 500, 1960, 14000$  GeV and the full lepton rapidity interval.

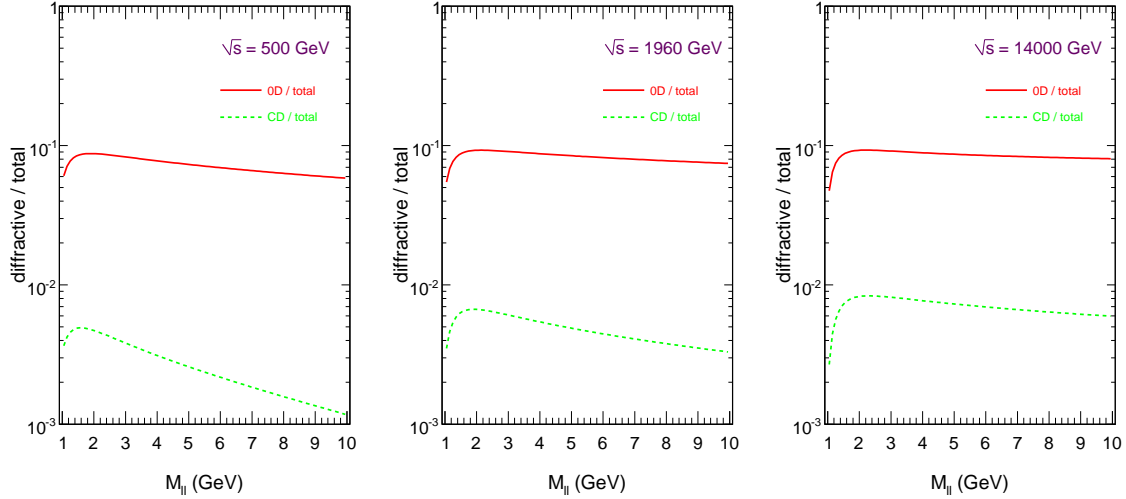


FIG. 5. Ratio of the single-diffractive DY (solid line) and central-diffractive DY (dashed line) cross section to the ordinary Drell-Yan cross section as a function of the dilepton invariant mass. The gap survival factors are not included in this plot and have to be taken into account in addition.

consequence of the cut imposed on the dilepton invariant mass  $M_{ll} > 1$  GeV, necessary to ensure validity of the perturbative calculation.

The rapidity distribution of the dilepton pair is shown in Fig.7. The distributions for the individual single diffractive mechanisms have maxima at large rapidities. When adding both single diffractive contributions we obtain distribution which has a shape similar to that for

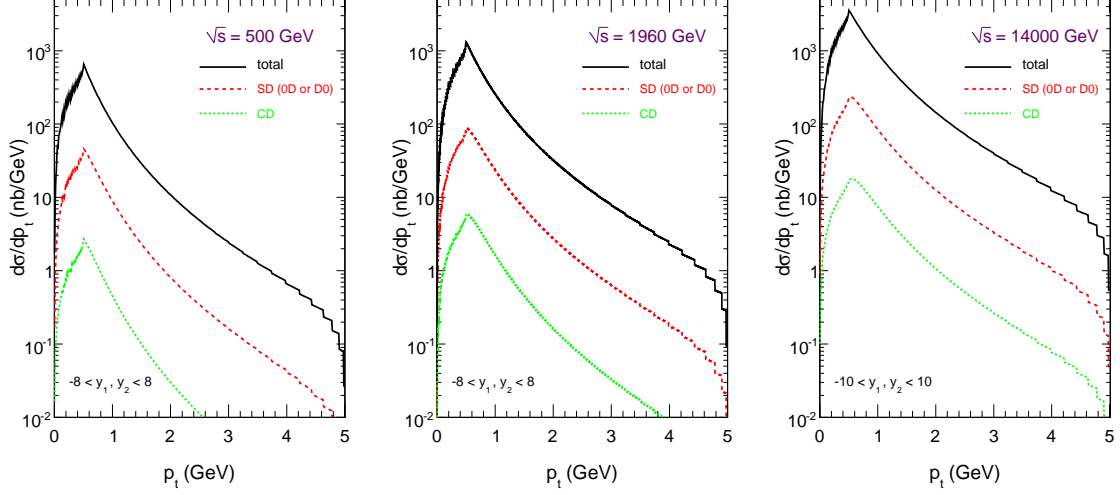


FIG. 6. Lepton transverse momentum distributions for the ordinary Drell-Yan (black line), single diffractive DY (dashed, red online) and central diffractive DY (dotted, green online). The results are shown for energies  $\sqrt{s}= 500, 1960, 14000$  GeV and the full lepton rapidity interval. Absorption effects are not included here.

the ordinary Drell-Yan. This means that the fraction of the single diffractive contribution is only weakly dependent on the lepton pair rapidity. The central diffractive contribution is concentrated at midrapidities. This is a consequence of limiting integration over  $x_{\mathbf{P}}$  in Eq.(2.6) to  $0.0 < x_{\mathbf{P}} < 0.1$ .

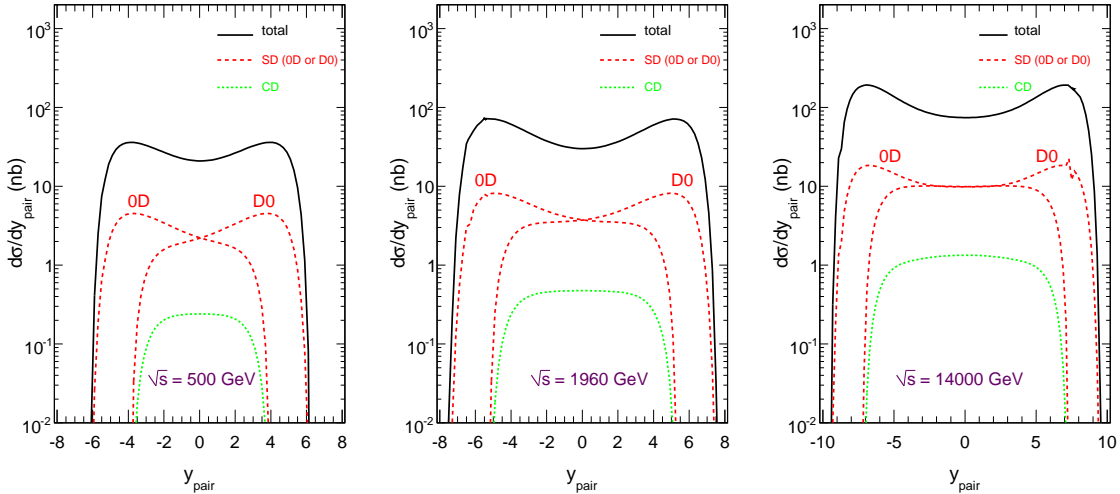


FIG. 7. Distribution in the lepton pair rapidity ( $y_{pair}$ ) for  $\sqrt{s}= 500, 1960, 14000$  GeV energy. Here  $M_{ll} > 1$  GeV. Absorption effects are not included here.

Now we wish to discuss some two-dimensional distributions. In Fig.8 maps in  $(M_{ll},$

$y_{pair}$ ) for the four different processes are presented. The shapes for different processes are somewhat different. In particular the distribution of the central-diffractive component is much narrower in the rapidity of the lepton pair.

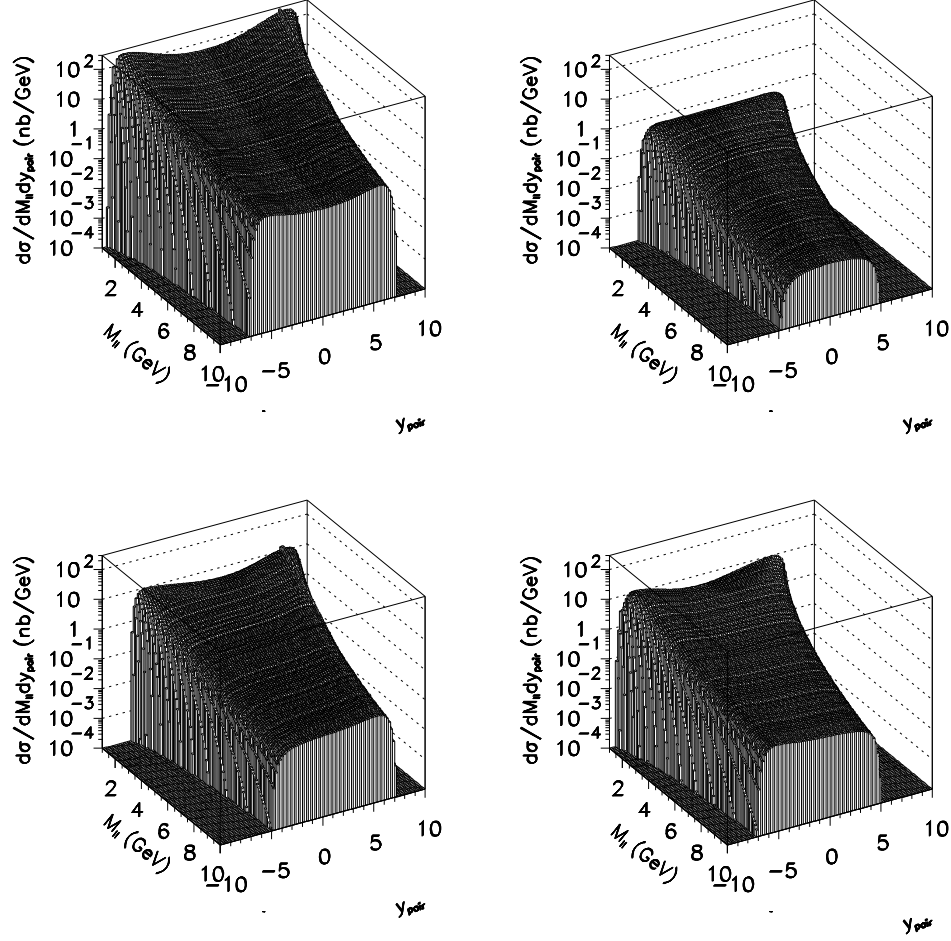


FIG. 8. Two-dimensional distributions in dilepton invariant mass  $M_{\ell\ell}$  and lepton pair rapidity  $y_{pair}$  for ordinary Drell-Yan (upper left panel), central diffractive DY (upper right panel) and single diffractive DY (lower panels) in  $pp$  collisions at  $\sqrt{s}=14000$  GeV. The cross sections for diffractive processes were not multiplied by the gap survival factors.

In Fig.9 we show correlations in lepton rapidities ( $y_1$  is for  $e^-$  and  $y_2$  is for  $e^+$ ). The distributions are concentrated along the diagonal  $y_1 = y_2$ . The distributions for individual single-diffractive components are peaked at large  $|y_1| \approx |y_2|$ . The LHC detectors have fairly large coverage in pseudorapidity for leptons so a measurement of such distributions in the near future is not excluded.

In the present paper we have calculated the cross section for single diffractive mechanism within a simple intuitive Ingelman-Schlein model [3]. We find that the ratio of the diffractive to the total cross section for dilepton pair production depends only slightly on kinematical variables: center-of-mass energy,  $M_{\ell\ell}$ ,  $y_{pair}$  or lepton transverse momenta. In Ref.[12] such ratio was calculated in the framework of the dipole approach to the Drell-Yan mechanism as



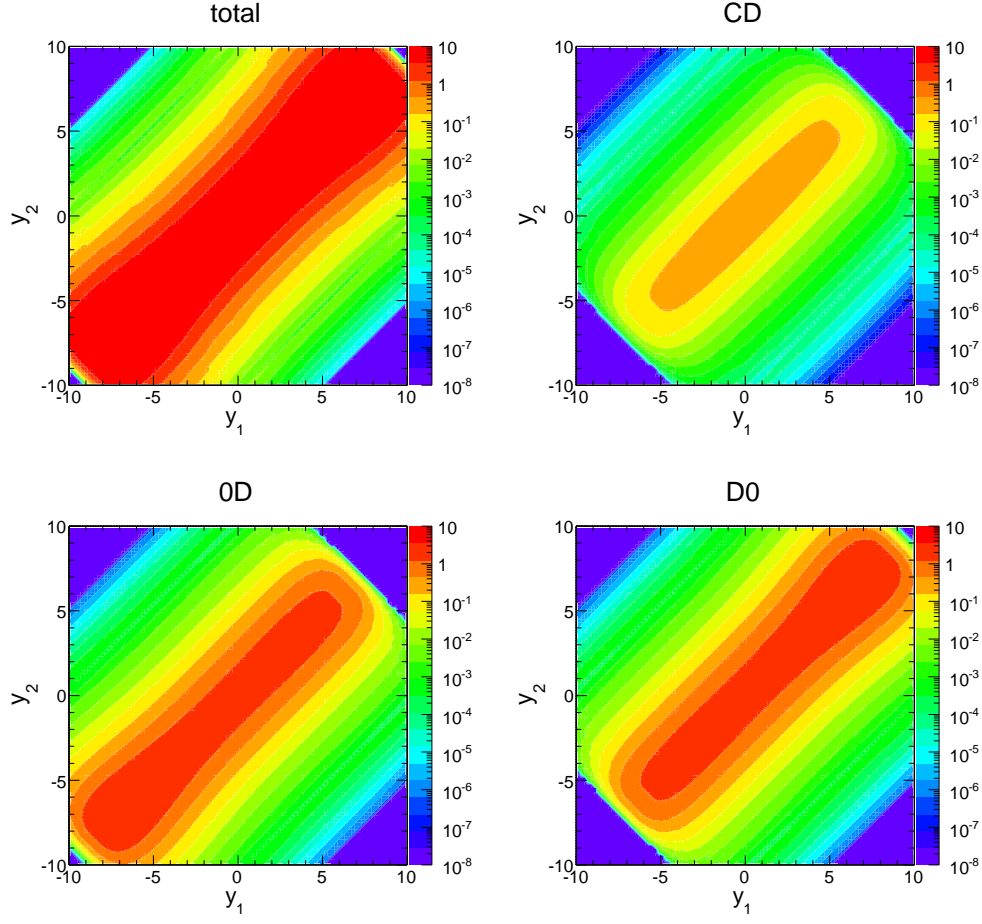


FIG. 9. Maps in  $y_1$  and  $y_2$  for the ordinary Drell-Yan (upper left panel), central diffractive DY (upper right panel) and single diffractive DY (lower panels) in  $pp$  collisions at  $\sqrt{s}=14000$  GeV. The cross sections for the diffractive processes were not multiplied by the gap survival factors.

a function of dilepton invariant mass for different center-of-mass energies. In this approach the ratio strongly decreases as a function of the center-of-mass energy and increases as a function of dilepton invariant mass. This is quite opposite to the present predictions, where the energy dependence of the ratio is rather slow and the ratio rather decreases as a function of the dilepton invariant mass.

### III. EXCLUSIVE PRODUCTION OF DILEPTONS

#### A. $pp \rightarrow pl^+l^-p$ via photon-pomeron subprocesses

Before we go to hadronic reaction let us start from recalling basic formula for the amplitude for exclusive photoproduction of lepton pairs in the  $\gamma p \rightarrow l^+l^-p$  reaction.

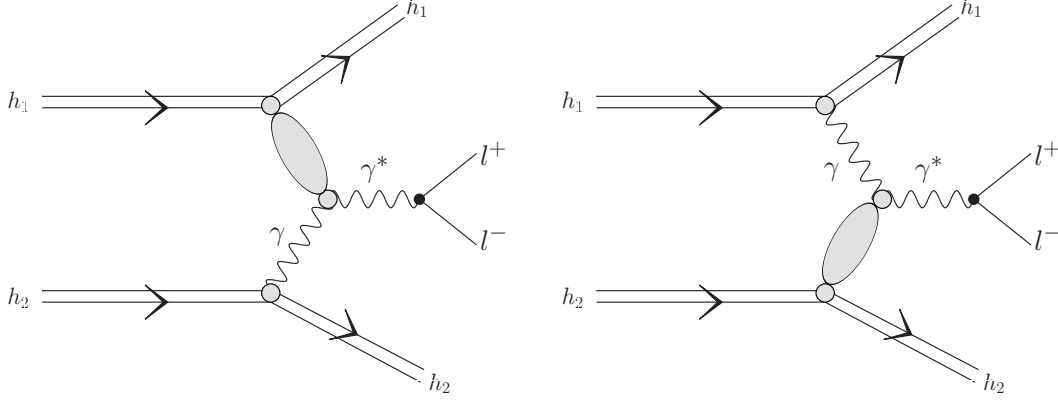


FIG. 10. An example of the non-QED mechanism for the production of opposite charge leptons in the  $pp \rightarrow ppl^+l^-$  reaction.

As shown in Ref.[16] the forward  $\gamma p \rightarrow \gamma^* p$  amplitude is a sum of amplitudes for a given flavor and the amplitude for a given flavour contribution can be written as:

$$\mathcal{M}_f(\gamma p \rightarrow \gamma^*(q^2)p) = W^2 4\pi\alpha_{\text{em}} e_f^2 2 \int_0^1 dz \int_0^\infty \pi dk_\perp^2 \frac{\mathcal{A}_f(z, k_\perp^2, W^2)}{[k_\perp^2 + m_f^2 - z(1-z)q^2 - i\varepsilon]}. \quad (3.1)$$

The real and imaginary part of the forward Time-like Compton Scattering (TCS) amplitude takes the form:

$$\begin{aligned} \Im \mathcal{M}_f(\gamma p \rightarrow \gamma^*(q^2)p) &= W^2 16\pi^2 \alpha_{\text{em}} e_f^2 \cdot \left\{ \theta(4m_f^2 - q^2) \int_{4m_f^2}^\infty dM^2 \frac{\Im a_f(W^2, M^2)}{M^2 - q^2} \right. \\ &\quad \left. + \theta(q^2 - 4m_f^2) \left( \text{PV} \int_{4m_f^2}^\infty dM^2 \frac{\Im a_f(W^2, M^2)}{M^2 - q^2} + \pi \Re a_f(W^2, q^2) \right) \right\}, \\ \Re \mathcal{M}_f(\gamma p \rightarrow \gamma^*(q^2)p) &= W^2 16\pi^2 \alpha_{\text{em}} e_f^2 \cdot \left\{ \theta(4m_f^2 - q^2) \int_{4m_f^2}^\infty dM^2 \frac{\Re a_f(W^2, M^2)}{M^2 - q^2} \right. \\ &\quad \left. + \theta(q^2 - 4m_f^2) \left( \text{PV} \int_{4m_f^2}^\infty dM^2 \frac{\Re a_f(W^2, M^2)}{M^2 - q^2} - \pi \Im a_f(W^2, q^2) \right) \right\}. \end{aligned} \quad (3.2)$$

where

$$a_f(W^2, M^2) = \frac{1}{M^2} \int_0^{\frac{1}{4}M^2 - m_f^2} \frac{dk_\perp^2}{J} \mathcal{A}_f(z(M^2, k_\perp^2), k_\perp^2, W^2). \quad (3.3)$$

Explicit formula for  $\mathcal{A}_f$  can be found in [16] where we also show its derivation as well as other details. The amplitude for the exclusive hadroproduction can be written schematically as

$$\begin{aligned}
\mathcal{M}_{pp \rightarrow ppl+l^-}^{\lambda_3 \lambda_4} &= eF_1(q_1^2)(\bar{u}_1 \gamma^\mu u_a) \left( \frac{-ig_{\mu\nu}}{t_1} \right) \Sigma_{\lambda_1} \epsilon^\nu(\lambda_1) \mathcal{M}_{\gamma p \rightarrow \gamma^* p}^{\lambda_1 \lambda_1'}(W_2, t_2, M_{ll}) \\
&\quad \Sigma_{\lambda_1'} \epsilon^{\alpha*}(\lambda_1') \left( \frac{-ig_{\alpha\beta}}{s_{34}} \right) e\bar{u}(\lambda_3, p_3) \gamma^\beta v(\lambda_4, p_4) \\
&\quad + eF_1(q_2^2)(\bar{u}_2 \gamma^\mu u_b) \left( \frac{-ig_{\mu\nu}}{t_2} \right) \Sigma_{\lambda_2} \epsilon^\nu(\lambda_2) \mathcal{M}_{\gamma p \rightarrow \gamma^* p}^{\lambda_2 \lambda_2'}(W_1, t_1, M_{ll}) \\
&\quad \Sigma_{\lambda_2'} \epsilon^{\alpha*}(\lambda_2') \left( \frac{-ig_{\alpha\beta}}{s_{34}} \right) e\bar{u}(\lambda_3, p_3) \gamma^\beta v(\lambda_4, p_4), \tag{3.4}
\end{aligned}$$

where  $\lambda_3, \lambda_4$  are helicities of  $l^+$  and  $l^-$ , respectively. Above  $M_{ll}$  is the invariant mass of the lepton pair,  $F_1$  is the Dirac electromagnetic form factor and  $\mathcal{M}_{\gamma p \rightarrow \gamma^* p}^{\lambda\lambda'}(W, t, M_{ll}) \propto \delta^{\lambda\lambda'}$  are amplitudes for the photon-proton subprocess discussed briefly above. In the present analysis we omit contributions related to the Pauli electromagnetic form factors. Their contribution in the integrated cross section is expected to be negligible.

Making further manipulations as in [17] we can write the four-body amplitude for the  $\gamma \mathbf{IP} + \mathbf{IP} \gamma$  exchanges in a somewhat simplified way

$$\begin{aligned}
\mathbf{M}_{pp \rightarrow ppl+l^-}^{\lambda_3 \lambda_4} &\approx \frac{2eF_1(t_1)\mathbf{q}_1}{z_1 t_1 \sqrt{1-z_1}} \sum_{\lambda_1} \mathcal{M}_{\gamma p \rightarrow \gamma^* p}^{\lambda_1}(W_2, M_{ll}) \epsilon_\mu^*(\lambda_1) \exp\left(\frac{B}{2}t_2\right) \frac{e}{M_{ll}^2} \bar{u}(p_3, \lambda_3) \gamma^\mu v(p_4, \lambda_4) \\
&\quad + \frac{2eF_1(t_2)\mathbf{q}_2}{z_2 t_2 \sqrt{1-z_2}} \sum_{\lambda_2} \mathcal{M}_{\gamma p \rightarrow \gamma^* p}^{\lambda_2}(W_1, M_{ll}) \epsilon_\mu^*(\lambda_2) \exp\left(\frac{B}{2}t_1\right) \frac{e}{M_{ll}^2} \bar{u}(p_3, \lambda_3) \gamma^\mu v(p_4, \lambda_4). \tag{3.5}
\end{aligned}$$

Above  $z_1$  and  $z_2$  are longitudinal momentum fractions of the intermediate space-like photons with respect to their parent protons and  $\mathbf{q}_1$  and  $\mathbf{q}_2$  are two-dimensional vectors related to the momentum transfer in the electromagnetic vertices. In the first exploratory calculation presented here we sum only over transverse photons, i.e.  $\lambda_1, \lambda_2 = \pm 1$ . The  $t$ -dependence of the amplitude is encoded in the exponential  $\exp(\frac{B}{2}t)$  form factor. The slope choice of the slope parameter  $B$  was discussed in Ref.[16].

The cross section is calculated as usually for a  $2 \rightarrow 4$  reaction:

$$\sigma = \int \frac{1}{2s} |\overline{\mathcal{M}}|^2 (2\pi)^4 \delta^4(p_a + p_b - p_1 - p_2 - p_3 - p_4) \frac{d^3 p_1}{(2\pi)^3 2E_1} \frac{d^3 p_2}{(2\pi)^3 2E_2} \frac{d^3 p_3}{(2\pi)^3 2E_3} \frac{d^3 p_4}{(2\pi)^3 2E_4}. \tag{3.6}$$

To calculate the total cross section one has to perform a 8-dimensional integral numerically. The details how to conveniently choose kinematical integration variables are explained in Ref.[18].

Some distributions initiated by the  $\gamma \mathbf{IP}$  or  $\mathbf{IP} \gamma$  subprocesses can be calculated with good precision in the equivalent photon approximation (EPA). A good example of such a distribution is

$$\frac{d\sigma}{dy_{pair} dM_{ll}} = \omega_1 \frac{dN_1(\omega_1)}{d\omega_1} \frac{d\sigma_{\gamma p \rightarrow l+l^- p}}{dM_{ll}}(W_2, M_{ll}) + \omega_2 \frac{dN_2(\omega_2)}{d\omega_2} \frac{d\sigma_{\gamma p \rightarrow l+l^- p}}{dM_{ll}}(W_1, M_{ll}). \tag{3.7}$$

Above  $\frac{dN_1}{d\omega_1}$  or  $\frac{dN_2}{d\omega_2}$  are photon fluxes in the first and second nucleon. Their explicit form can be found e.g. in [19]. The differential distributions  $\frac{d\sigma}{dM_{ll}}$  were calculated and shown in Ref. [16]. We have found that the EPA distributions are almost identical with corresponding ones obtained for the four-body reaction as discussed above.

### B. $pp \rightarrow pl^+l^-p$ via photon-photon fusion

Here we present a formalism necessary for the calculation of the amplitude and cross section for the photon-photon fusion. The basic mechanism is shown in Fig.11.

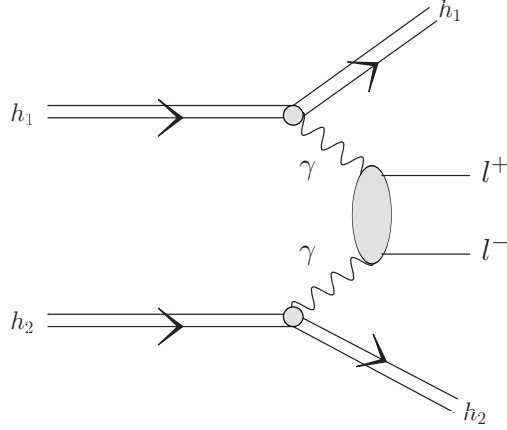


FIG. 11. The QED  $\gamma\gamma$  fusion mechanism of the exclusive lepton production.

The amplitude for the two-photon  $2 \rightarrow 4$  process shown in Fig.11 can be written as:

$$\begin{aligned} \mathcal{M}_{\lambda_a \lambda_b \rightarrow \lambda_1 \lambda_2 \lambda_3 \lambda_4}^{pp \rightarrow pp l^+ l^-} &= \bar{u}(p_1, \lambda_1) \Gamma_1^{\mu_1}(q_1) u(p_a, \lambda_a) \\ &\left( \frac{-ig_{\mu_1 \nu_1}}{t_1} \right) V_{\lambda_3 \lambda_4}^{\nu_1 \nu_2}(q_1, q_2, p_3, p_4) \left( \frac{-ig_{\mu_2 \nu_2}}{t_2} \right) \\ &\bar{u}(p_2, \lambda_2) \Gamma_2^{\mu_2}(q_2) u(p_b, \lambda_b), \end{aligned} \quad (3.8)$$

where presented below factor describes the production amplitude of a  $l^+l^-$  pair with helicities  $\lambda_3, \lambda_4$  and momenta  $p_3, p_4$ , respectively

$$V_{\lambda_3 \lambda_4}^{\nu_1 \nu_2}(q_1, q_2, p_3, p_4) = e^2 \bar{u}(p_3, \lambda_3) \left[ \gamma^{\nu_1} \frac{\hat{q}_1 - \hat{p}_3 - m}{(q_1 - p_3)^2 - m^2} \gamma^{\nu_2} - \gamma^{\nu_2} \frac{\hat{q}_1 - \hat{p}_4 + m}{(q_1 - p_4)^2 - m^2} \gamma^{\nu_1} \right] v(p_4, \lambda_4).$$

$\Gamma_1^{\mu_1}(q_1)$  and  $\Gamma_2^{\mu_2}(q_2)$  are vertex functions describing coupling of virtual space like photon to the nucleon, which can be expressed by the well-known electromagnetic Dirac and Pauli form factors of the proton as:

$$\Gamma_1^{\mu_1}(q_1) = \gamma^{\mu_1} F_1(q_1) + \frac{i\kappa_p}{2M_p} \sigma^{\mu_1 \nu_1} q_{\nu_1} F_2(q_1), \quad (3.9)$$

$$\Gamma_2^{\mu_2}(q_2) = \gamma^{\mu_2} F_1(q_2) + \frac{i\kappa_p}{2M_p} \sigma^{\mu_2\nu_2} q_{\nu_2} F_2(q_2) , \quad (3.10)$$

where

$$\begin{aligned} \sigma^{\mu\nu} &= \frac{i}{2}(\gamma^\mu\gamma^\nu - \gamma^\nu\gamma^\mu), \\ q_1 &\equiv p_1 - p_a, \\ q_2 &\equiv p_2 - p_b. \end{aligned} \quad (3.11)$$

Using the Gordon decomposition one can simplify the tensorial structure

$$\Gamma_1^{\mu_1}(q_1) = (F_1(q_1) + \kappa F_2(q_2))\gamma^{\mu_1} - \frac{\kappa F_2(q_1)}{2m_N}(p_a + p_1)^{\mu_1} , \quad (3.12)$$

$$\Gamma_2^{\mu_2}(q_2) = (F_1(q_2) + \kappa F_2(q_2))\gamma^{\mu_2} - \frac{\kappa F_2(q_2)}{2m_N}(p_b + p_2)^{\mu_2} . \quad (3.13)$$

As for the diffractive case in the present paper we neglect contributions related to the Pauli form factors which are very small for the integrated cross section.

### C. Results

In this section we shall present results for exclusive diffractive mechanism discussed above. We shall show differential cross sections for  $\mu^+\mu^-$  production via  $\gamma\mathbf{IP}$  or  $\mathbf{IP}\gamma$  exchange and for comparison via  $\gamma\gamma$  fusion<sup>2</sup>. Here we shall concentrate on the LHC energy  $\sqrt{s}=14$  TeV. Let us start from the dilepton invariant mass distribution shown in Fig.12. The diffractive contribution is about two-orders of magnitude smaller than that for the photon-photon fusion. The shape of the distribution is rather similar. We do not include here absorption effects neither for the  $\gamma\gamma$  nor for the  $\gamma\mathbf{IP}$  ( $\mathbf{IP}\gamma$ ). In both cases they are rather small (see e.g. [17]).

As for the inclusive case we also show distribution for lepton pair rapidity. The diffractive component is in addition decomposed into separate contributions corresponding to  $\gamma\mathbf{IP}$  fusion (right bump) and  $\mathbf{IP}\gamma$  fusion (left bump). It can be shown that without absorption effects the two contributions add incoherently in the lepton pair rapidity<sup>3</sup>.

In Fig.14 we present azimuthal correlations between the outgoing leptons for the  $\gamma\gamma$  fusion (dashed line) and for the  $\gamma\mathbf{IP} + \mathbf{IP}\gamma$  exchanges (solid line). Azimuthal angle distribution for the  $\gamma\gamma$  process peaks sharply at  $\phi \sim 180^\circ$  but for the  $\gamma\mathbf{IP} + \mathbf{IP}\gamma$  process leptons prefer to go into the same hemisphere. This distribution could be therefore used for imposing cuts in order to enhance the contribution of the new diffractive photoproduction mechanism.

In all the distributions presented above the  $\gamma\gamma$  mechanism dominates over the diffractive one. Can the diffractive mechanism be identified experimentally? The leptons in  $\gamma\gamma$  process are emitted preferentially back-to-back and their transverse momenta almost cancel. This means that for this process transverse momentum of the pair should be small. It is not necessarily so for the diffractive mechanism where the transverse momentum kick to a

<sup>2</sup> In contrast to inclusive diffractive DY the cross section for exclusive production of  $e^+e^-$  pairs is significantly bigger than that for  $\mu^+\mu^-$  production.

<sup>3</sup> This is not true for other distributions, in particular for azimuthal angle correlations between outgoing protons (see e.g. [17]).

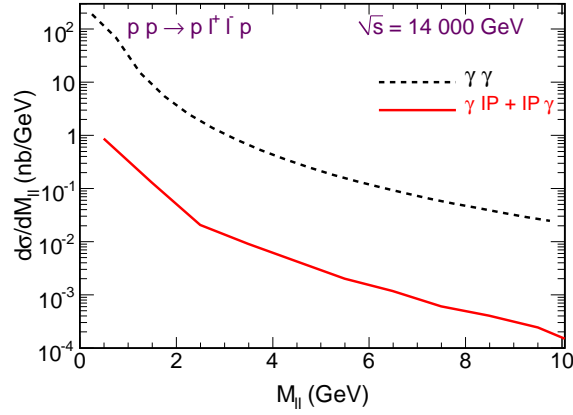


FIG. 12. Dependence of the cross section on the dilepton invariant mass for the  $\gamma\gamma$  (dashed line) and for the diffractive mechanism (solid line).

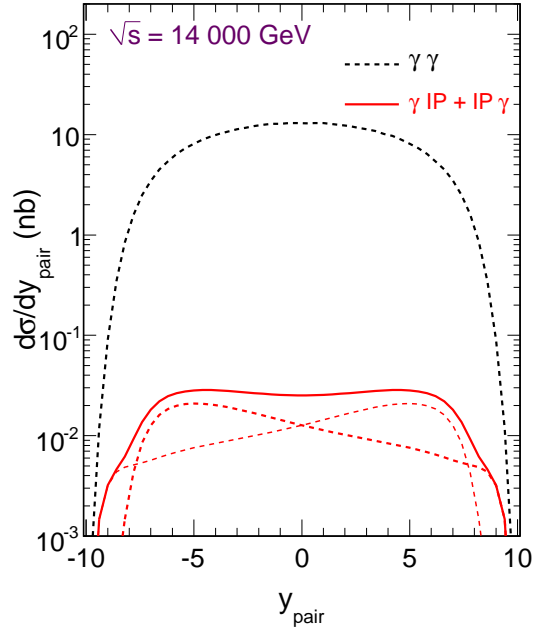


FIG. 13. Lepton pair rapidity distribution for the  $\gamma\gamma$  (dashed line) and for the diffractive mechanism (solid line) which is further decomposed into  $\gamma\mathbf{IP}$  and  $\mathbf{IP}\gamma$  contributions.

proton due to the pomeron (gluonic ladder) exchange is much bigger than that due to photon exchange. In Fig.15 we show distribution in transverse momentum of the dilepton pair ( $\vec{p}_{t,sum} = \vec{p}_{1t} + \vec{p}_{2t}$ ). As expected the photon-photon contribution dominates at small transverse momenta of the pair, while the photon-pomeron (pomeron-photon) contributions at transverse momenta larger than about 1 GeV. We therefore think that imposing a cut on the

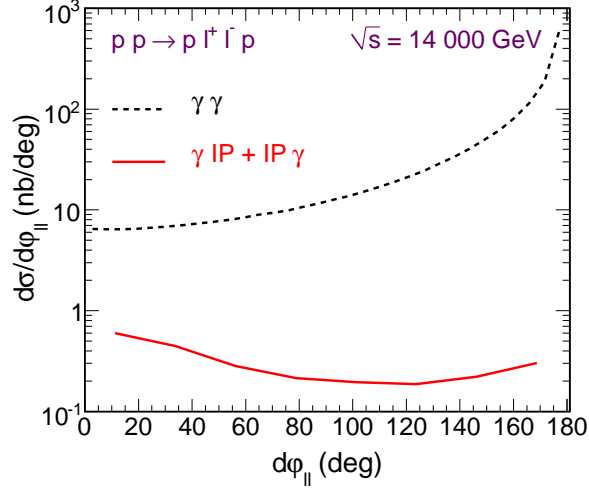


FIG. 14. Distribution in relative azimuthal angle between outgoing leptons.

variable would be useful and perhaps necessary to identify the diffractive photoproduction mechanism.

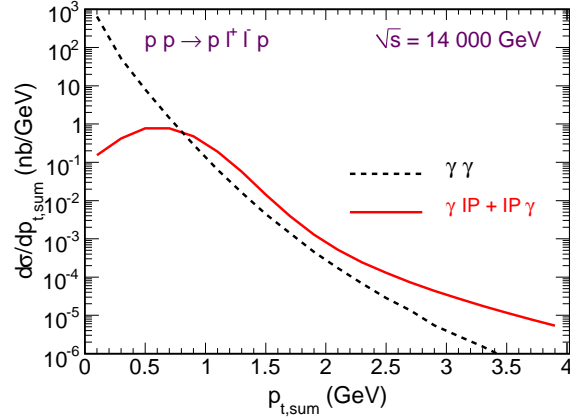


FIG. 15. Dependence on the transverse momentum of the dilepton pair ( $p_{t,sum}$ ) for the diffractive (solid line) and photon-photon (dashed line) contributions.

Can we further “pin down” the photoproduction mechanism? Let us consider now two-dimensional correlations for outgoing particles. Let us start with correlations between transverse momenta of outgoing protons. Since transverse momenta of outgoing protons are rather small (photon or pomeron exchange) we shall use  $\xi_1 = \log_{10}[p_{1t}/1 \text{ GeV}]$  and  $\xi_2 = \log_{10}[p_{2t}/1 \text{ GeV}]$  instead of transverse momenta. In Fig.16 we show two-dimensional correlations in the  $(\xi_1, \xi_2)$  space. Different pattern can be seen for the  $\gamma\gamma$  and diffractive mechanisms. It is not clear to us at present if the measurement of transverse momenta of protons will be precise enough to impose cuts in the two-dimensional space.

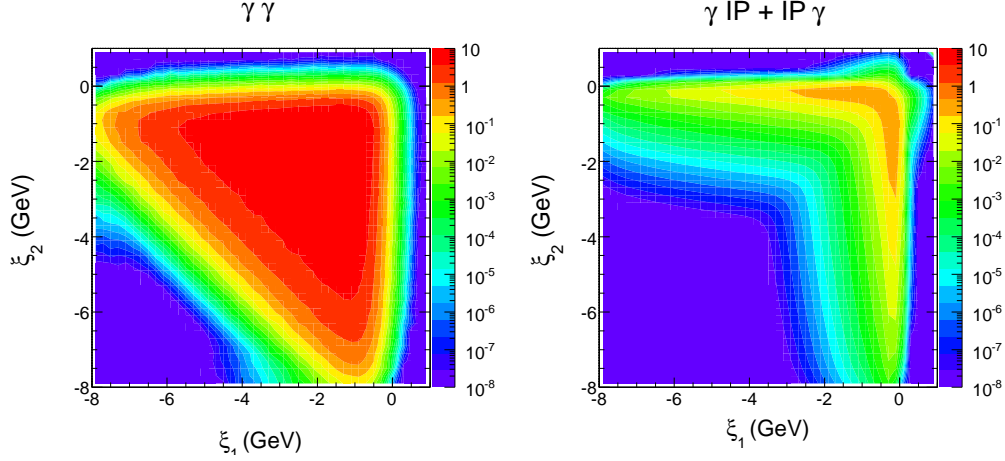


FIG. 16. Transverse momentum correlations of outgoing protons for the  $\gamma\gamma$  fusion (left panel) and for the  $\gamma\mathbf{IP} + \mathbf{IP}\gamma$  exchange (right panel).

We do similar analysis for transverse momenta of outgoing muons. Fig.17 shows two-dimensional distribution in transverse momentum of outgoing leptons. A strong correlation between transverse momentum of the negative and positive muon can be seen. The further from the diagonal the bigger fractional contribution of the diffractive mechanism. We conclude that this figure contains essentially similar information as the distribution in transverse momentum of the dilepton pair shown in Fig.15.

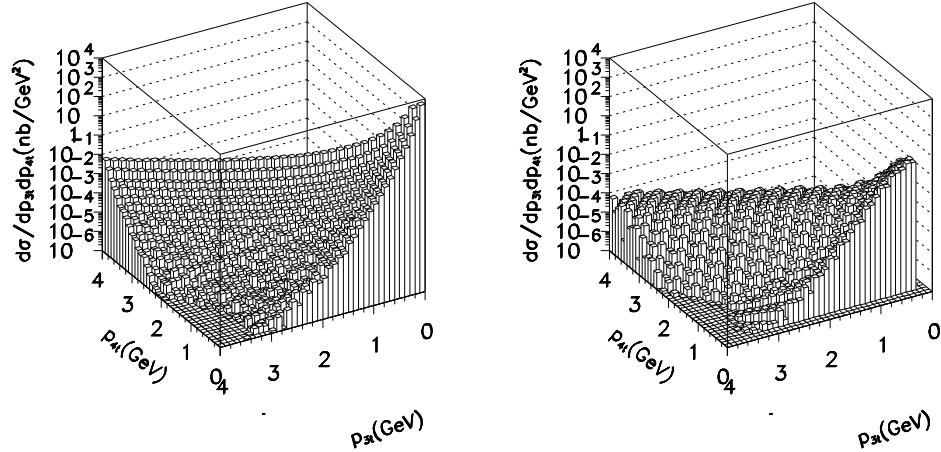


FIG. 17. Correlations in transverse momenta of outgoing leptons for the  $\gamma\gamma$  fusion (left panel) and for the  $\gamma\mathbf{IP} + \mathbf{IP}\gamma$  exchange (right panel).

In analogy to the inclusive case we consider correlations in the lepton rapidity space. The situation on the two-dimensional plane  $(y_3, y_4)$  is shown in Fig.18 for the  $\gamma\gamma$  fusion (left panel) and for the  $\gamma\mathbf{IP} + \mathbf{IP}\gamma$  exchange (right panel). We observe that the correlations for



the diffractive mechanism are stronger than that for the  $\gamma\gamma$  fusion. Therefore one could impose further cut on the difference of the lepton rapidities:  $y_{diff} \equiv y_3 - y_4$ .

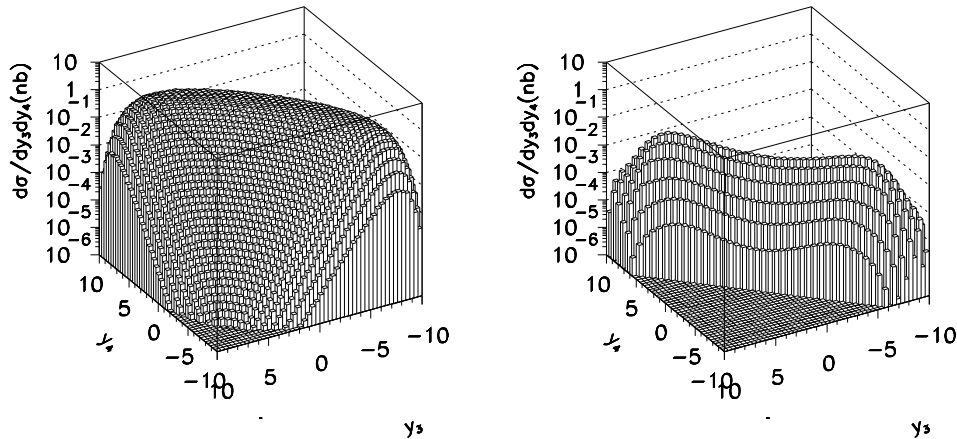


FIG. 18. Rapidity correlations of leptons for the  $\gamma\gamma$  fusion (left panel) and for the  $\gamma\mathbf{IP} + \mathbf{IP}\gamma$  exchange (right panel).

How big are cross sections for the exclusive mechanisms discussed in this section in comparison to those for inclusive cross sections calculated in the Ingelman-Schlein model corrected for absorption. In Fig.19 we have collected lepton pair rapidity distributions for different processes: ordinary nondiffractive Drell-Yan, single and central diffractive Drell-Yan, exclusive production of dilepton pair via the  $\gamma\gamma$  fusion and via  $\gamma\mathbf{IP} + \mathbf{IP}\gamma$  exchange. In this plot we include absorption effects discussed in the previous section. We observe that the cross section for the  $\gamma\gamma$  mechanism is larger than that for the single and central diffractive ones. On the other hand, the cross section for exclusive diffractive production is only slightly smaller than that for the central diffractive mechanism.

Further studies are clearly needed in order to demonstrate whether measurements of the cross section of the discussed mechanisms are possible.

#### IV. CONCLUSIONS

We have calculated distributions in lepton rapidity, lepton transverse momentum as well as dilepton invariant mass for inclusive single and central diffractive production of dileptons in proton-proton collisions. In this calculations we have used diffractive parton distributions found from the analysis of the proton diffractive structure function and dijet production in deep inelastic scattering. The distributions have been compared with the corresponding distributions for ordinary nondiffractive Drell-Yan process. The distribution in rapidity for the single-diffractive process is very similar to that for the nondiffractive case. The single diffractive mechanism constitutes about a percent of the inclusive mechanism. The cross section for central diffractive mechanism is smaller than that for single diffractive one by one order of magnitude.

In our approach the ratio of the diffractive to the total cross section for the dilepton production only slightly depends on the center-of-mass energy and the dilepton mass. This

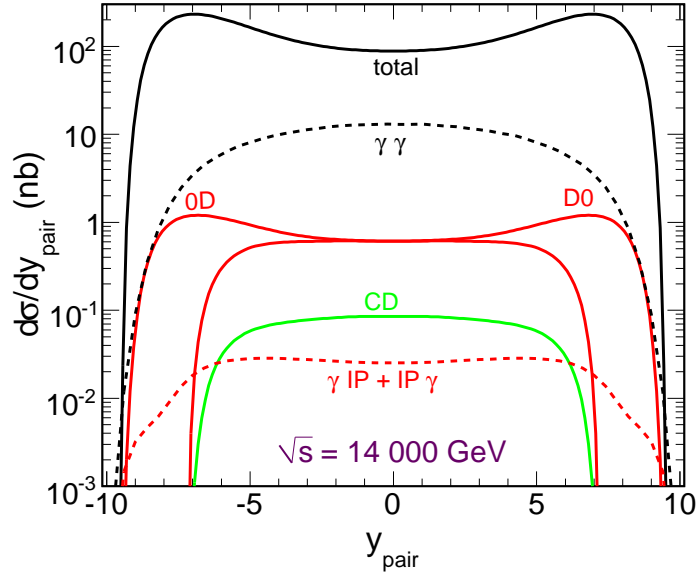


FIG. 19. Distribution in lepton pair rapidity for all processes considered in the present paper at the nominal LHC energy  $\sqrt{s}=14\,000$  GeV. The inclusive diffractive processes are shown by the solid lines and the exclusive ones by the dashed lines. Here we have included gap survival factors as explained in the text.

is in evident contrast to earlier predictions made within the dipole approach. Experimental studies would clearly shed more light on the issue and would help in understanding the diffractive mechanism in hadronic processes, certainly not fully understood so far.

We have also calculated several differential distributions for exclusive diffractive production of dileptons. Here the photon-pomeron (pomeron-photon) is the driving mechanism. We have applied here a formalism used previously for the  $\gamma p \rightarrow l^+ l^- p$  reaction.

This formalism was previously successfully tested for exclusive production of vector mesons. The distributions for the diffractive exclusive process were compared with corresponding distributions for the QED photon-photon mechanism. We have found regions of the phase space where the diffractive mechanism dominates over the QED one. Several differential distributions have been shown and discussed. Experimental identification of the exclusive diffractive process is very important in the context of the proposal to use the QED photon-photon fusion to monitor luminosity at the LHC. Clearly further Monte Carlo studies are necessary.

## Acknowledgments

This work was partially supported by the MNiSW grants: N202 2492235 and N N202 236937. A discussion with Wolfgang Schäfer and his collaboration on the dilepton production in the  $\gamma p \rightarrow l^+ l^- p$  reaction as well as a discussion with Poman Pasechnik is kindly

acknowledged.

- 
- [1] G. Fai, J. Qiu and X. Zhang, Phys.Rev.**C71** (2005) 014901.
  - [2] P. Bruni, G. Ingelman, Phys.Lett.**B311** 317 (1993);  
L. Alvero, J.C. Collins, J. Terron and J.J. Whitmore, Phys. Rev. **D59** (1999) 074022;  
R.J.M. Covolan and M.S. Soares, Phys. Rev. **D60** (1999) 054005, Phys. Rev. **D67** (2003) 017503;  
M.B. Gay Ducati, M.M. Machado and M.V.T Machado, Phys. Rev. **D75** (2007) 114013.
  - [3] G. Ingelman, P.E. Schlein, Phys.Lett.**B152** 256 (1985).
  - [4] M.B. Gay Ducati, M.M. Machado and M.V.T Machado, Phys. Rev. **D81** (2010) 054034;  
M. Heyssler, Z. Phys. **C73** (1997) 299.
  - [5] R. Enberg, G. Ingelman, N. Timneanu, Phys.Rev.**D67** (2003) 011301;  
S. Erhan, V.T. Kim and P.E. Schlein,[arXiv:hep-ph/0312342];  
M.B. Gay Ducati, M.M. Machado and G.G. Silveira,[arXiv:hep-ph/1101.5602].
  - [6] A. Berera, J.C. Collins, Nucl. Phys. **B474** 183 (1996);  
R.J.M. Covolan and M.S. Soares, Phys. Rev. **D67** (2003) 077504.
  - [7] M.V.T. Machado, Phys. Rev. **D76** (2007) 054006.
  - [8] A. Cisek, W. Schäfer and A. Szczurek, Phys. Rev. **D80** (2009) 074013.
  - [9] A. Aktas *et al.* [H1 Collaboration], Eur. Phys. J. C **48**, 715 (2006) [arXiv:hep-exp/0606004].
  - [10] A.G. Shamov and V.I. Telnov, Nucl. Instr. and Meth. **A 494** (2002) 51;  
K. Piotrkowski, Proposal for luminosity measurement at LHC. ATLAS note PHYS-96-077, 1996, unpublished;  
D. Bocian and K. Piotrkowski, Acta Phys. Polon. **B 35** (2004) 2417;  
M.W. Krasny, J. Chwastowski, K. Słowikowski, Nucl. Instr. and Meth. **A 584** (2008) 42;  
X. Rouby, PhD Thesis 2008 Measurements of photon induced processes of CMS and forward photon detection at the LHC.
  - [11] M. Khusek, W. Schäfer, A. Szczurek, Phys.Lett. **B674** 92 (2009).
  - [12] B.Z. Kopeliovich, I.K. Potashnikova, I. Schmidt, A.V. Tarasov, Phys.Rev.**D74** (2006) 114024, e-Print: hep-ph/0605157.
  - [13] V. Barger and R. Phillips, "Collider Physics", Addison-Wesley Publishing Company, Redwood Cite, 1987.
  - [14] V.A. Khoze, A.D. Martin and M.G. Ryskin, Eur. Phys. J. **C18**, 167 (2000).
  - [15] U. Maor, AIP Conf. Proc. **1105**, 248 (2009).
  - [16] W. Schäfer, G. Ślipek, A. Szczurek, Phys.Lett.**B688** 158 (2010).
  - [17] W. Schäfer and A. Szczurek, Phys. Rev. **D76** (2007) 094014.
  - [18] P. Lebiedowicz and A. Szczurek, Phys. Rev. **D81** (2010) 036003.
  - [19] M. Drees and D. Zeppenfeld, Phys. Rev. **D39** (1989) 2536.